DOI: 10.1002/chem.200902596

Aggregation and Contingent Metal/Surface Reactivity of 1,3,8,10-Tetraazaperopyrene (TAPP) on Cu(111)

Manfred Matena,[a] Meike Stöhr,*[a] Till Riehm,[c] Jonas Björk,[e] Susanne Martens,[c] Matthew S. Dyer,[e] Mats Persson,[e, f] Jorge Lobo-Checa,[a, b] Kathrin Müller,[d] Mihaela Enache,[a] Hubert Wadepohl,[c] Jörg Zegenhagen,[g] Thomas A. Jung,*[d] and Lutz H. Gade*[c]

Abstract: The structural chemistry and reactivity of 1,3,8,10-tetraazaperopyrene (TAPP) on Cu(111) under ultra-high-vacuum (UHV) conditions has been studied by a combination of experimental techniques (scanning tunneling microscopy (STM) and X-ray photoelectron spectroscopy, XPS) and DFT calculations. Depending on the deposition conditions, TAPP forms three main assemblies, which result from initial submonolayer coverages based on different intermolecular interactions: a close-packed assembly similar to a projection of the bulk structure of TAPP, in which the molecules interact mainly through van der Waals (vDW) forces and weak hydrogen bonds; a porous copper surface coordination network; and covalently linked molecular chains. The Cu substrate is of crucial importance in determining the structures of the aggregates and available reaction channels on the surface, both in the formation of the porous network for which it provides the Cu atoms for surface metal coordination and in the covalent coupling of the TAPP molecules at elevated temperature. Apart from their role in the kinetics of surface transformations, the available metal adatoms may also profoundly influence the thermodynamics of transformations by coordination to the reaction product, as shown in this work for the case of the Cu-decorated covalent poly(TAPP–Cu) chains.

Keywords: aggregation · C–H activation · coordination networks · density functional calculations · surface chemistry

Introduction

The recent interest in organic nanostructures on surfaces[1,2] emerged from their prospective applications in nanoscale electronic or optoelectronic devices[3] in which the spatially addressable functional units are assembled at the molecular level. By combining established methods of molecular and supramolecular synthesis[4] with the remarkable capabilities of surface microscopy and analytics,[5] along with recently developed theoretical modelling tools,[6] several strategies

[a] M. Matena, Dr. M. Stöhr, Dr. J. Lobo-Checa, M. Enache
NCCR Nanoscale Science and Department of Physics
University of Basel, Klingelbergstr. 82, 4056 Basel (Switzerland)
Fax: (+41) 612673784
E-mail: meike.stoehr@unibas.ch

[b] Dr. J. Lobo-Checa
Current address: Centre d'Investigaciò en Nanociència
i Nanotecnologia CIN2 (CSIC-ICN)
Esfera UAB, Campus de la UAB, 08193-Bellaterra (Spain)

[c] Dr. T. Riehm, S. Martens, Prof. H. Wadepohl, Prof. Dr. L. H. Gade
Anorganisch-Chemisches Institut, Universität Heidelberg
Im Neuenheimer Feld 270, 69120 Heidelberg (Germany)
Fax: (+49) 6221545609
E-mail: lutz.gade@uni-hd.de

[d] Dr. K. Müller, Dr. T. A. Jung
Laboratory for Micro- and Nanotechnology, Paul-Scherrer-Institute
5232 Villigen (Switzerland)
Fax: (+41) 563102646
E-mail: thomas.jung@psi.ch

[e] J. Björk, Dr. M. S. Dyer, Prof. M. Persson
Surface Science Research Centre
Department of Chemistry, University of Liverpool
Crown Street, Liverpool, L69 7ZD (UK)

[f] Prof. M. Persson
Department of Applied Physics
Chalmers University of Technology, 412 96 Gothenburg (Sweden)

[g] Dr. J. Zegenhagen
European Synchrotron Radiation Facility
38043 Grenoble, Cedex 9 (France)

 © 2010 Wiley-VCH Verlag GmbH & Co. KGaA, Weinheim WILEY InterScience DISCOVER SOMETHING GREAT

towards that goal have emerged. Well-defined surface assemblies have been obtained by condensation of organic molecules from the vapour phase at the solid/vacuum interface[7] or from solutions at the solid/liquid interface.[8] Molecules of variable dimensions and levels of functionality on well-defined crystal surfaces of the coinage metals (in particular) have been studied.[9] It is the balance between intermolecular and molecule–surface interactions, the reversibility or irreversibility of intermolecular bond formation and the resulting availability or non-availability of structural repair mechanisms that governs the detailed structures and long-range order of molecular surface assemblies.[10]

Whereas weak intermolecular interactions such as vdW forces and hydrogen bonding have been shown to lead to molecular arrays characterised by high levels of long-range order and tunable structural characteristics[11] such as porosity,[12] their generally observed thermal instability limits this approach in the fabrication of hierarchically assembled aggregates. Surface coordination networks obtained either by combination of organic ligands with adatoms of the substrate or by their reaction with vapour-deposited heterometal atoms possess greater inherent stability.[13,14] However, the closed-shell[15] interactions representing the coordinative metal–ligand bonds may be readily broken at elevated temperature and are both thermodynamically and kinetically less stable than the covalent bonds (shared interactions)[15] within the organic building blocks. Such covalent bond formation on metal surfaces has been reported only recently[2,16] and may occur either by classical condensation of suitable precursors[17] or by thermal generation of activated species that couple subsequently to oligomeric or polymeric structures.[18,19] The latter may provide access to reaction patterns and transformations that are not available in wet chemical synthesis and the investigation of contingent metal/surface reactivity of organic molecules is thus of particular interest.

Recently we reported the synthesis of 1,3,8,10-tetraazaperopyrene (TAPP),[20] a condensed poly-N-heterocyclic aromatic compound, which contains four potentially metal-ligating exodentate N-donor functions that are symmetrically arranged with respect to the principal molecular axis (Figure 1). Additionally, the C–H bridge between the two nitrogen atoms offers the potential of tautomerisation to an N-heterocyclic carbene isomer, or may undergo metal-induced C–H activation at elevated temperatures. In both cases, highly reactive molecular fragments would result that could recombine to give covalently linked TAPP oligomers or polymers.[19]

This inter-relationship of molecular properties and contingent reactivity makes TAPP an ideal object of study, not only to probe previously formulated concepts of surface-confined supramolecular chemistry, but to obtain new insights into the way in which a metal substrate with its mobile surface adatoms at elevated temperatures may chemically activate organic molecules for potential covalent coupling. Here we present an account of the structural chemistry and reactivity of TAPP on Cu(111) that addresses the patterns of aggregation and reactivity in different regimes of thermal energy.

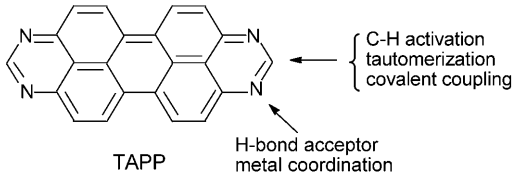

Figure 1. 1,3,8,10-Tetraazaperopyrene (TAPP) and its potential for 2D interactions on surfaces.

Results and Discussion

Three-dimensional (3D) bulk structures and two-dimensional (2D) surface structures of organic molecules are not necessarily directly related because the intra- and intermolecular degrees of freedom of their components differ. However, the simple plate-like molecular shapes and the limited variability of stacking motifs of polycyclic aromatic molecules[21] may make it possible to relate 2D projections of the crystal structure with weakly aggregated surface arrays of these species provided that the molecule substrate interactions are not dominating the intermolecular interactions. This has been found to be the case for TAPP. With the crystal structure as a point of reference, the behaviour of TAPP on a Cu(111) surface within different temperature regimes will be discussed.

Crystal structure of TAPP: TAPP crystals suitable for X-ray diffraction were obtained by sublimation in a temperature-programmed tube furnace (440→250 °C) at ambient pressure under a stream of nitrogen as the carrier gas.

In the crystal the molecules adopt a typical herringbone arrangement.[21] The angle between the principal molecular axes in neighbouring stacks is 58.0° (Figure 2, left), a mutual

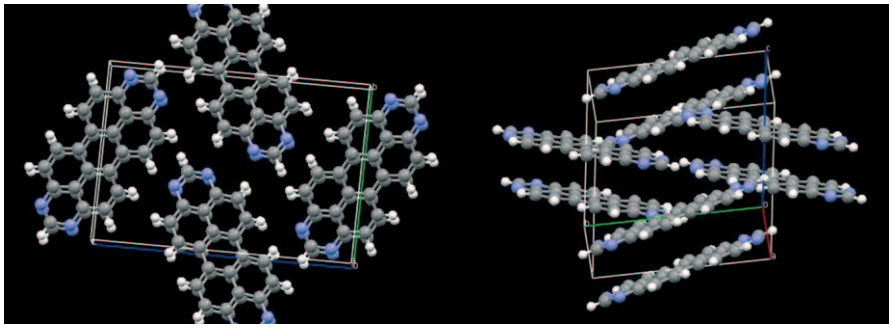

Figure 2. Stacking of the TAPP molecules in the single crystal: left, view along the *a* axis of the monoclinic unit cell, illustrating the relative orientation of the principal molecular axes of neighbouring stacks; right, relative tilt of the stacking aromatic polycycles.

 © 2010 Wiley-VCH Verlag GmbH & Co. KGaA, Weinheim

orientation of the molecules that is essentially retained upon their deposition on Cu(111) surfaces, as will be discussed below. Within the individual stacks the molecules are superposed along [100] with the molecular planes parallel to one another but tilted with respect to the (100) crystal plane. The molecular stacks are crosslinked by weak CH···N hydrogen bonding (CH···N 2.56, 2.45 Å refined C–H distances; or 2.47, 2.35 Å for C–H distances normalised to 1.083 Å).[22] The π–π interplanar distance of 3.37 Å is close to that of graphite (3.35 Å).[23]

Low-temperature deposition and aggregation of TAPP on a Cu(111) surface: Upon deposition of TAPP at a substrate temperature of −110 °C, the observed formation of aggregates (clusters, Figure 3a) indicates an attractive intermolecular interaction.

When the substrate temperature is raised to −90 °C for deposition of TAPP, patches of an ordered close-packed assembly (Figure 3c) could be observed first; their detailed structure is displayed in Figure 3e). The unit cell was determined by STM to be $(17\pm1.7)\times(12\pm1.2)$ Å^2 with an angle of $(84\pm4)°$. According to the corresponding tentative model for this 2D array (Figure 3b), the molecules interact through weak vdW forces and weak hydrogen bonding, forming an assembly that is related to the crystal structure of TAPP discussed in the previous section. The angle between the principal molecular axes in neighbouring braids is $(54\pm7)°$ and thus is in the same range as the analogous parameter in the crystal structure (see above). This similarity between the crystal structure of a molecule and its assembly on the surface was found for, amongst other examples the perylene derivative perylene tetracarboxyanhydride (PTCDA).[24] One reason for the formation of patches, characterised by their extension in the order of 5–10 nm, instead of large homogeneous islands may be a possible lattice mismatch between the molecular adlayer and the substrate. This notion is consistent with the rather weak intermolecular (vdW) interactions, which have to compete with the interaction between molecule and substrate. Another reason might be that the chosen substrate temperature (−90 °C) is too low to induce the rearrangement of unordered preformed clusters into larger ordered arrays, as is evidenced by the observed formation of larger islands upon annealing at −45 °C (Figure 3d). A systematic investigation of this aspect was precluded by the emergence at higher temperatures of new types of surface assemblies that compete with (and finally supersede) the weakly interacting herringbone structure. This transformation into ordered molecular-surface networks based on stronger intermolecular interactions will be discussed in the following section.

Formation of a tetragonal surface coordination network: A highly ordered, porous network (Figure 4) becomes the dominating structure upon deposition of TAPP at higher substrate temperatures or upon thermal annealing of the low-temperature phase. This assembly is interpreted as a coordination polymer in which the lone pairs of the nitrogen of TAPP coordinate to Cu adatoms as indicated in the structural model depicted in Figure 4b. As will be shown below, this interpretation is consistent with the total energy calculations of the system. Whereas the formation of such coordination oligomers is already observed after annealing of the low-temperature phase at 0 °C, the full conversion into the porous network is achieved at 150 °C. Both deposition of TAPP at this temperature and thermal annealing of the preformed low-temperature phase allow the formation of large and homogeneous islands as shown in Figure 4a.[19]

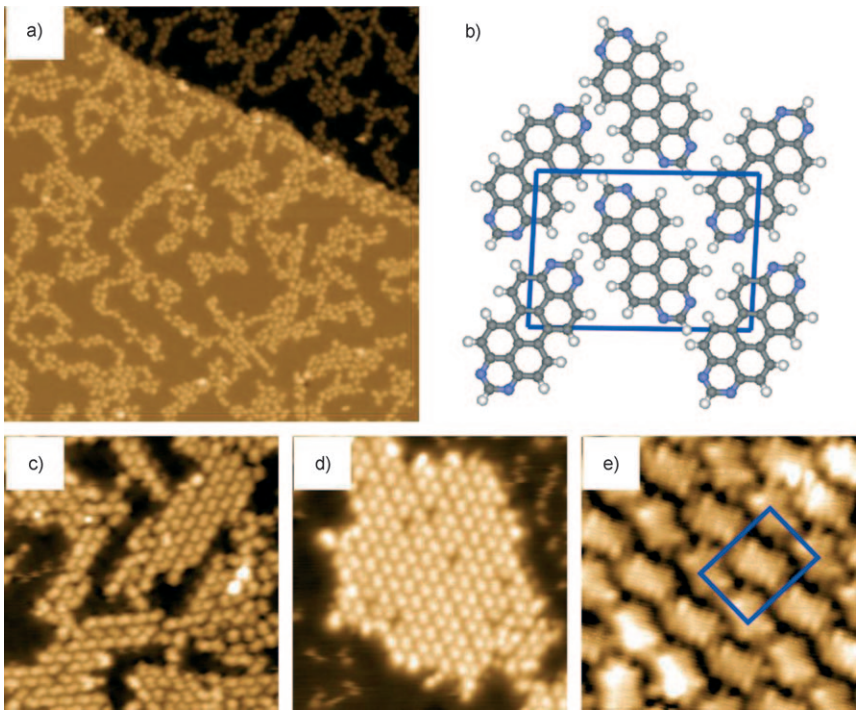

Figure 3. STM images of TAPP deposited on Cu(111): a) mostly disordered and irregularly shaped admolecular islands after deposition at a substrate temperature of −110 °C (66×66 nm^2, −1.5 V/12 pA); b) tentative model corresponding to the unit cell superimposed on (e); c) first ordered patches of a close-packed assembly after deposition at a substrate temperature of −90 °C (18×18 nm^2, −0.7 V/20 pA); d) formation of larger islands after annealing at −45 °C (17×17 nm^2, −1.5 V/20 pA); e) the close-packed assembly in detail (5×5 nm^2, −0.8 V/90 pA) after annealing at +40 °C.

The analysis of the low-energy electron diffraction (LEED) data (Figure 4c–e) supports a commensurate superstructure of the molecular

 © 2010 Wiley-VCH Verlag GmbH & Co. KGaA, Weinheim

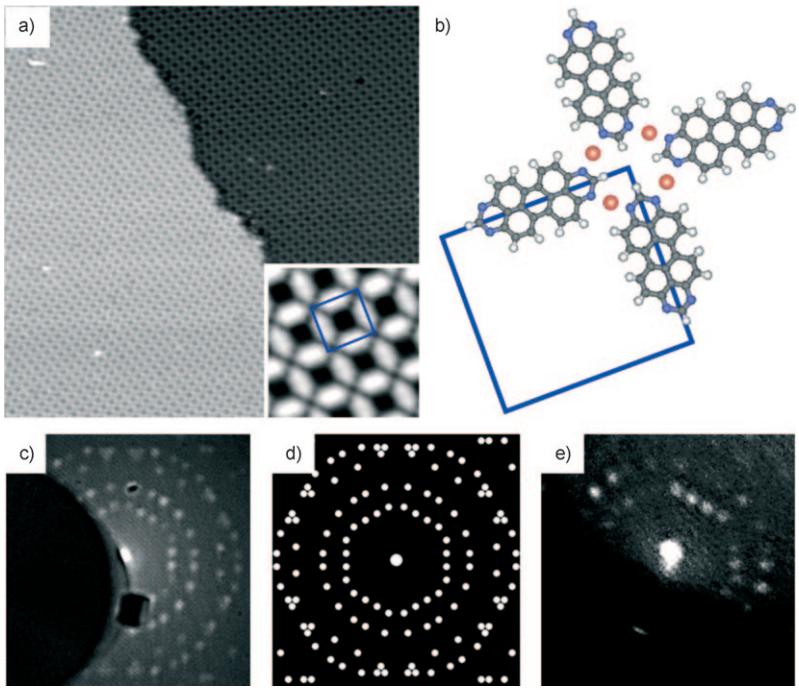

Figure 4. a) STM image of TAPP deposited on Cu(111) at a sample temperature of 150 °C (70×70 nm^2, −1.4 V/20 pA). The inset (lower right) shows the porous structure in detail (5.3×5.3 nm^2, −0.4 V/20 pA). b) Proposed structure of the porous network. c) LEED pattern of the porous network (beam energy = 29.5 eV). d) Simulated LEED pattern for comparison (see ref. [25]). e) Zoom-in to first-order spot of the Cu crystal. The LEED pattern was taken at 52 eV.

$$\begin{pmatrix} 8 & 5 \\ 1 & 6 \end{pmatrix}$$

adlayer on the substrate. The matrix of the molecular adlayer[26] was found to be given by the matrix shown on the left.

Apart from the very good reproduction of the LEED pattern (Figure 2c) by the simulation (Figure 4d) by using the above matrix, there are two further aspects that support a commensurate adlayer: On the one hand, very large homogeneous islands of TAPP (significantly larger than 100 nm^2) could be observed on the Cu surface. On the other, the molecular LEED pattern around the (00) spot (Figure 4c) is reproduced at the first-order LEED spot of the Cu substrate (Figure 4e).

The fact that the molecular layer is commensurate with the underlying Cu substrate does not necessarily imply that the threefold symmetry of the underlying substrate has to result in threefold symmetry of the molecular layer. A well-established example is the pattern of aggregation of PTCDA on Ag(111), for which an almost rectangular unit cell is observed that is commensurate with the Ag substrate.[24]

Role of the metal adatoms for the stability of the surface coordination network: The Cu adatoms between the molecules of the porous network could not be identified directly by STM, so their role in stabilisation of the observed Cu/TAPP surface coordination network was assessed by a computational study in which DFT methods were used (Figure 5). A molecular arrangement representing a local energetic minimum, which is stabilised by weak C–H···N hydrogen bonding enabled by slightly rotating the molecules, was chosen as the non-metalated reference structure (Figure 5b).

The porous network was theoretically modelled with and without Cu adatoms present (Figure 5) by working within the unit cell determined by LEED. Our calculations showed that the porous network is stabilised by coordination to Cu adatoms. The geometry of the TAPP molecule prevents the coordination of the four nitrogen atoms directly to the bare Cu(111) surface, because to obtain a reasonable bond angle the molecule would have to bend and twist significantly. Instead, in the absence of Cu adatoms, rather weak CH···N hydrogen bridges are formed between the molecules (Figure 5b). The adsorption energy of this non-metalated structure was found to be −0.33 eV molecule^{-1} relative to an isolated relaxed TAPP molecule plus the relaxed Cu-

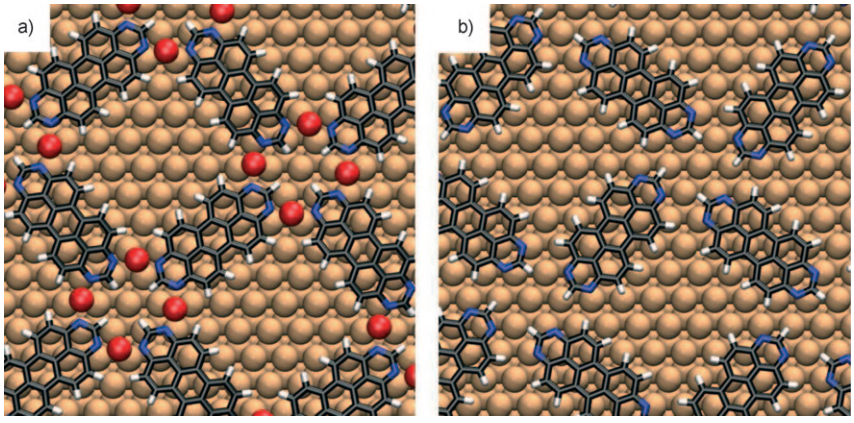

Figure 5. Calculated minimal-energy structures of the porous network of TAPP on Cu(111) a) with and b) without adatoms. In the latter case the molecules interact through C–H···N hydrogen bonds. The DFT calculations show that the metal-coordinated structure (a) is energetically favoured.

 © 2010 Wiley-VCH Verlag GmbH & Co. KGaA, Weinheim

(111) surface (a negative adsorption energy indicates a stabilisation of the system relative to the reference systems). Because Cu adatoms are raised above the surface, N–Cu bonds can be formed without significant twisting or bending of the molecule. By introduction of four Cu adatoms per crossing between four TAPP molecules (equivalent to two adatoms per TAPP molecule) a porous network coordinated to the Cu adatoms is formed (Figure 5a). The adsorption energy of this metal-coordinated network was found to be $-2.40\ eV\,molecule^{-1}$ relative to an isolated relaxed TAPP molecule plus the relaxed Cu(111) surface with four adatoms (see the Computational Studies section for a detailed description of how the adsorption energies were calculated). This structure is considerably energetically favoured over the non-metalated structure even if the energy cost for the creation of free adatoms from a step edge of 0.76 eV per adatom[27] is taken into account. The N–Cu distance (2.06 Å computed from the relaxed structure) agrees well with the values known from Cu coordination chemistry.[28]

Observation of a second surface structure at submonolayer coverage: A second close-packed structure (assembly 2 in Figure 6a) is observed, in addition to the low-temperature structure (assembly 1 in Figure 6a) and the porous network (Cu/TAPP = assembly 3 in Figure 6a), at annealing temperatures and times that are low enough to prevent the exclusive formation of the porous network, but high enough to activate Cu coordination. The intermolecular interactions in assembly 2 in Figure 6a are also postulated to be based upon Cu coordination (see Figure 6b). Because this more densely spaced array is expected to prevail over the porous network (assembly 3 in Figure 6a) at coverages higher than the maximum TAPP coverage required for the porous network, all experiments were performed at submonolayer coverage to investigate its relationship with the other two ordered assemblies. Under these conditions the porous network discussed in the preceding section was found to be the thermodynamically favoured form of aggregation.

A detailed analysis of the STM images of assembly 2 in Figure 6, considering different domains together with the symmetry of the substrate, results in two independent unit cells that do not overlap if rotations and mirror operations are constrained to those allowed by the symmetries of the substrate. Based on the dimensions of both the unit cell and the metric parameters of the TAPP molecules, the overall N–Cu–N distance was found to be 4 Å (that is, Cu–N = 2 Å), which is again consistent with the established coordination chemistry of copper.[28] At submonolayer coverage the fraction of molecules arranged according to this structure never exceeded 15% of the overall number of molecules forming the three ordered structures (Figure 6a).

Supply of Cu adatoms for the surface coordination network: In recent years there have been major research efforts directed towards the formation and characterisation of metal–organic surface coordination networks (MOCNs),[13,14,29] both by co-deposition of metal atoms[30] and by coordination of organic ligands to free adatoms on Cu(100) and Cu(111).[29,31,32] In the latter case, the reservoir of Cu adatoms has been discussed as resulting primarily from detachment and re-attachment of Cu atoms from and to step edges.[31,32] Whereas the formation of surface coordination networks on Cu(100) is already observed at room temperature (RT),[32] the formation of such structures on Cu(111) has been reported only at elevated temperatures of around 150 °C.[31] Furthermore, Schunack et al. have observed the formation of Cu nanostructures below molecules on Cu(110) at ambient temperature, mainly at step edges and very rarely on terraces.[33a] The latter effect has been related to the low concentration of Cu adatoms at room temperature, whereas the formation of nanostructures (both at steps and on terraces) was thought to be thermally activated. According to Giesen, the concentration of adatoms on Cu surfaces at room temperature is of the order of 10^{-9} per surface atom.[34] This is far too low to account for the formation of significant levels of surface coverage of coordination networks. Therefore, the temperature-dependent detachment/attachment rate of adatoms is important because it determines the time the system requires to respond to a perturbation of the equilibrium concentration of free adatoms caused by their coordination to organic molecules.[33b]

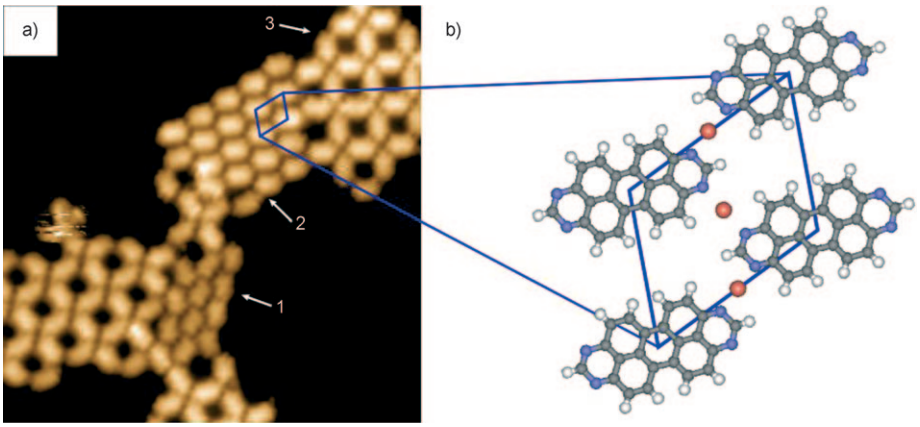

Figure 6. a) STM image of TAPP on Cu(111) after annealing at 80 °C, showing the close-packed assembly driven by vdW interactions and weak H bonding 1, a second close-packed assembly 2 and the porous network 3 driven by metal coordination ($17 \times 17\ nm^2$, –1.2 V/20 pA). b) Proposed model of assembly 2.

In view of the previously reported Arrhenius dependence of the detachment/attachment rate of adatoms from/to kinks on Cu(111),[27] the observation of large assemblies based on Cu coordination after annealing at temperatures around or slightly above room temperature is an

 © 2010 Wiley-VCH Verlag GmbH & Co. KGaA, Weinheim

unexpected result. Comparison of the number of Cu atoms expected to detach from kinks according to Giesen et al.[27] with the number of atoms needed to form the metal-coordinated assemblies raises the question of further possible mechanisms for the supply of Cu atoms required for the formation of the Cu/TAPP coordination network(s).

It has been shown that at 600 K the mass transport on Cu(111) at step edges is dominated by the exchange of atoms with the neighbouring terrace, whereas the dominating mass transport at temperatures below 500 K is by diffusion along steps.[27,35] The latter temperature range is relevant for the formation of the metal-coordinated assemblies in our case and might explain the affinity of TAPP network patches formed in close proximity to step edges. Note that step decoration of TAPP already occurs at low temperatures (Figure 7). This suggests that TAPP is mobile before enough

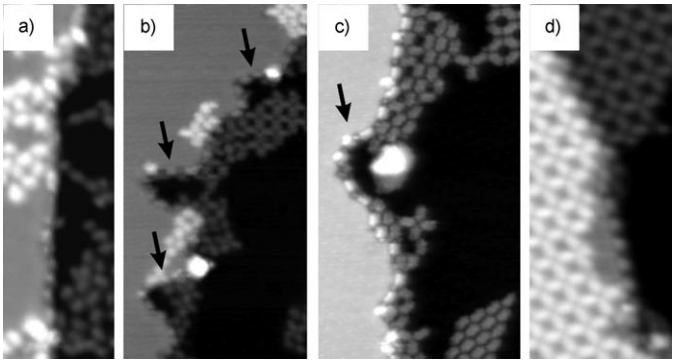

Figure 7. Step reorganisation and decoration after annealing the sample at different sample annealing temperatures: a) −110 °C (6×19 nm^2, −1.5 V/12 pA); b) RT (19×36 nm^2, −1.3 V/20 pA). c) RT (15×27 nm^2, −1.3 V/20pA); d) 150 °C (9×23 nm^2, −1.4 V/20 pA); e) 240 °C (12×22 nm^2, −1.1 V/20 pA). The black arrows highlight bays at the steps that are decorated by TAPP molecules.

metal adatoms are available, and it is preferentially attached to the step edges as reported for other molecular adsorbates containing planar π systems. The observation of bays at RT (Figure 7b and c) is an indication of the ability of the TAPP molecules to remove adatoms from step edges.[29] In other words, specific edge or kink sites are releasing metal atoms, which subsequently form networks by bonding to the mobile TAPP molecules. Thus, TAPP is thought to have a corrosive effect on the steps of the substrate, either directly by interaction with the step adsorption site, or indirectly because of its presence and diffusibility on the extended terraces. The previously reported formation of Cu nanostructures below molecules at steps supports this interpretation, because their strong affinity for metal atoms induces the detachment of Cu atoms from steps.[33]

Thermal degradation of the surface coordination network: We previously reported that annealing of the Cu/TAPP coordination network at about 250 °C leads to the formation of covalently bonded chains.[19] This thermally induced formation of macromolecules has been interpreted in terms of the tautomerisation of the N-heterocyclic end units of the TAPP molecules to carbene intermediates, iso-TAPP, which couple according to a Wanzlick-type dimerisation.[36] Although this postulated reaction pathway avoids high-energy intermediates that would result from the direct C–H bond cleavage and the subsequent recombination of radical intermediates, the latter cannot be ruled out (see below). The curved arrangement of some chains, indicating that their orientation is not determined by the substrate lattice structure, along with the possibility of mechanically manipulating the oligomer chains as a whole, provides additional support for the model of covalently linked TAPP molecules.[19]

There appears to be arbitrary arrangement of the TAPP chains on the Cu(111) surface (Figure 8a). However, the observed orientations of the chains with respect to the principal directions of Cu(111) were statistically analysed to uncover the possible influence of the surface on their alignment. Samples with low molecular coverage were used for this study to minimise interactions between chains. The resulting histogram (Figure 8b) shows the alignment of 178

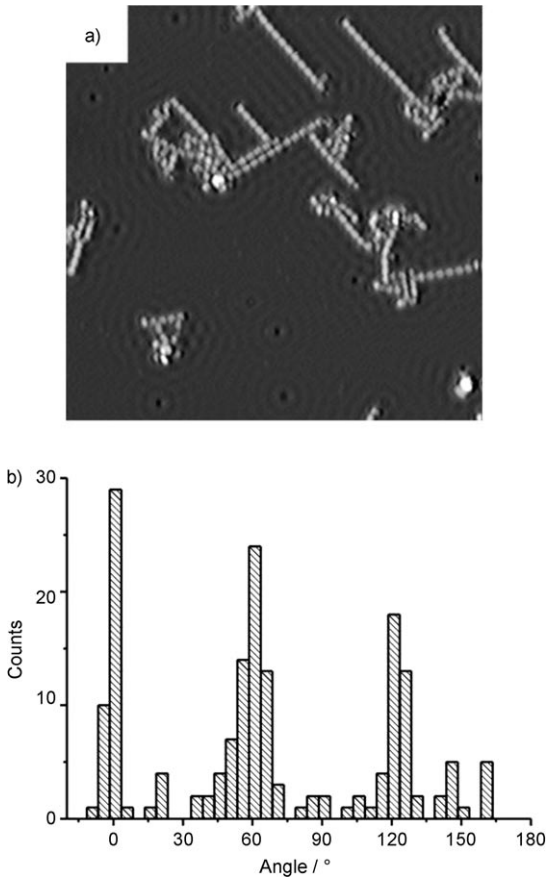

Figure 8. a) STM image of the TAPP chains at low coverage (50×50 nm^2, −0.1 V/20 pA). Owing to the low tunnelling voltage used to acquire this STM image, standing-wave patterns in the Shockley surface state of Cu(111) can be observed as they arise from scattering at chains as well as defects (see refs. [37], [38]). b) Histogram showing the directions of alignment of 178 chains at low coverage. An STM image with atomic resolution of the Cu substrate was used for calibration so that 0° corresponds to one of the high-symmetry directions of the Cu substrate.

 © 2010 Wiley-VCH Verlag GmbH & Co. KGaA, Weinheim

chains. It exhibits three pronounced orientations differing by 60°, which match the hexagonal symmetry of the (111) surface. An STM image with atomic resolution of the Cu substrate confirmed that the statistically favoured orientations indeed correspond to the high-symmetry directions of the surface structure. Both the distance of 12.7 Å between the centroids of adjacent monomer units in the chain, as determined by (gas-phase) theoretical modelling,[19] and the STM result of (12 ± 1.2) Å closely correspond to the five-fold distance of the lattice constant of the (111) surface (5×2.56 Å = 12.8 Å). This would allow a commensurate arrangement of the majority of the chains with the substrate, a situation that may be energetically favoured. However, we note that a significant number of chains are not aligned along the high-symmetry directions, indicating that the bonding between the monomer units in oligomeric molecules clearly dominates over the interaction with the metal surface.

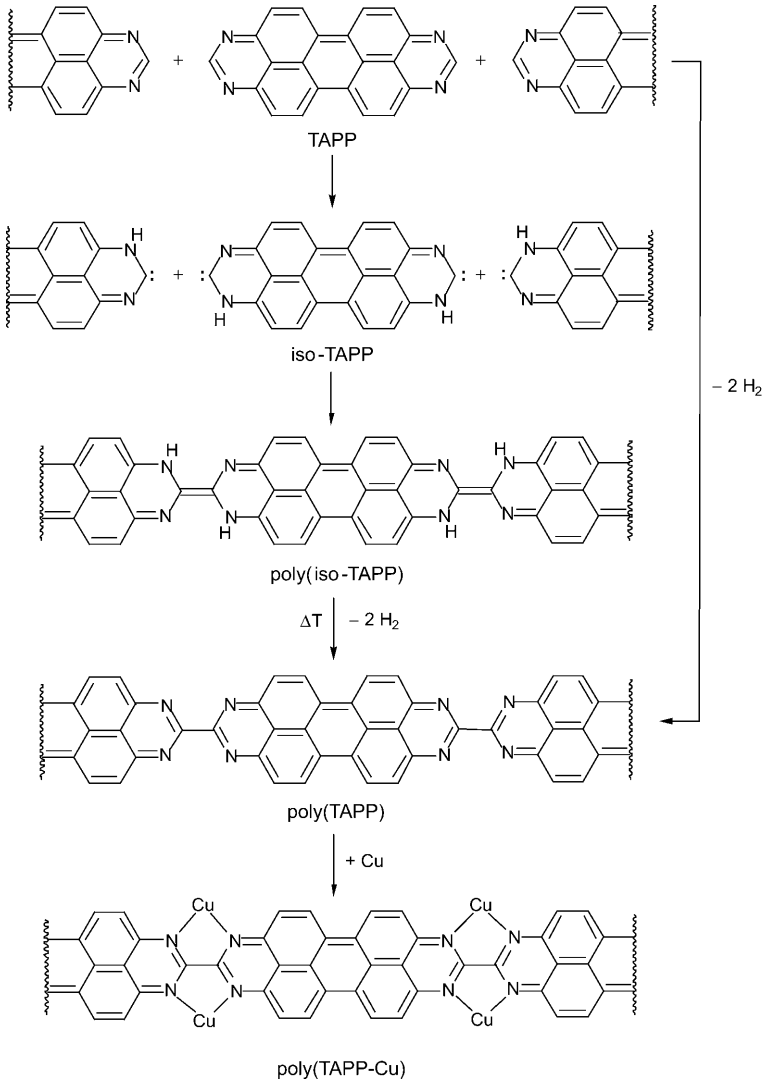

Scheme 1. Simplified scheme of the proposed surface-mediated transformation of TAPP to poly(TAPP) and its metal-decorated form, poly(TAPP–Cu).

Chemical nature of the $(TAPP)_n$ chains: The proposed chemical nature of the polymeric chains generated in the surface thermolysis of the Cu/TAPP network structure, along with two potential intermediates of two reaction pathways for their generation, is summarised in Scheme 1. In analogy with a growing number of reported examples of N-heterocycles isomerising to their N-heterocyclic carbene tautomers within the coordination sphere of transition metals,[39] TAPP molecules could undergo a metal-mediated rearrangement to iso-TAPP on the copper surface and subsequently combine in a Wanzlick-type coupling to the oligomeric chains poly(iso-TAPP) observed in our study. Whereas such a reaction sequence would be energetically unfavourable for simple N-heterocycles, a recent DFT study of the process in the gas phase has shown that the process would be exothermic for condensed poly(heterocycle)s such as TAPP.[19] It is likely that the iso-TAPP intermediates would be stabilised by C coordination to Cu adatoms on the metal surface in analogy to the large number of established stable copper complexes of N-heterocyclic carbenes, thus providing a low-energy pathway to poly(iso-TAPP).[40] However, our inability to date to obtain direct evidence for this conjecture is unsurprising, because single Cu–iso-TAPP species are expected to be indistinguishable by STM from non-rearranged TAPP molecules (also see the STM study on metalated poly(TAPP) discussed below).

We previously noted that there was evidence, based on the observed metalation of the polymer chains by Cu adatoms, that the chain structures detected by STM had undergone a dehydrogenation step subsequent to the coupling which results in poly(TAPP) (Scheme 1). Such a thermal dehydrogenation on Cu(111) has been observed for a perylene derivative.[41] Theoretical modelling of a process of this kind established it as being endothermic both in the gas phase and on the copper surface (see below). However, as will be shown below, the metalation of the resulting polydentate surface ligand that gives poly(TAPP–Cu) would make the overall process energetically favourable.

 © 2010 Wiley-VCH Verlag GmbH & Co. KGaA, Weinheim

An alternative reaction path, which is indicated in Scheme 1 for the polymerisation, could be based on a direct C–H bond activation and recombination of the resulting radicals. Such a high activation energy reaction pathway has been postulated in a recent report on the surface polymerisation of porphyrins.[18b] On the basis of the available experimental data, we are not able to distinguish between these two alternative routes resulting in the same polymer structures.

Although the reaction pathway leading to the TAPP chains could not be established with the available theoretical and experimental tools, we focused on detailed identification of the polymeric structures in particular, to distinguish between the three possibilities represented in Scheme 1: poly(iso-TAPP), the dehydrogenated poly(TAPP) and its metal-decorated form poly(TAPP–Cu).

To obtain an insight into the energetics of the proposed processes leading to the chains on the Cu surface, a DFT surface-modelling study was carried out to compare the viability of these three alternatives (Scheme 2), the results of which are summarised in Table 1. To obtain the overall conversion energies for the three processes, isolated relaxed TAPP molecules and the relaxed Cu substrate (with adatoms for the adatom coordinated structure) were used as reference systems. To model the dehydrogenation step involved in the formation of poly(TAPP) and poly(TAPP–Cu), a separate calculation of atomic hydrogen adsorbed on Cu(111) was performed and the energy was included in the overall conversion energies (see the Computational Studies section for a detailed description of how the reaction energies were calculated).

$$\mathrm{TAPP_{(g)} \xrightarrow{Cu(111)} poly(iso\text{-}TAPP)_{(ad)}}$$

$$\mathrm{TAPP_{(g)} \xrightarrow{Cu(111)} poly(TAPP)_{(ad)} + 2H_{(ad)}}$$

$$\mathrm{TAPP_{(g)} \xrightarrow{Cu(111)+2\,Cu} poly(TAPP\text{-}Cu)_{(ad)} + 2H_{(ad)}}$$

Scheme 2. The three overall processes compared in the DFT surface modelling study.

Both poly(iso-TAPP) and the adatom-coordinated poly(TAPP–Cu) chains are energetically favoured with respect to the reference system, whereas the formation of poly(TAPP) is clearly disfavoured. The generation of Cu adatoms from steps at 0.76 eV per atom[27] would reduce the exothermicity of the poly(TAPP–Cu) chain. However, the breakdown of the copper surface coordination network, along with the elevated temperatures needed for the polymerisation ($T \approx 250\,^{\circ}\mathrm{C}$), should provide a sufficient supply with Cu adatoms (see above).[27]

Table 1. Calculated overall reaction energies of three different types of chains.

Type of chain	E_{react} [eV molecule^{-1}]
poly(iso-TAPP)	−1.12
poly(TAPP)	+0.29
poly(TAPP–Cu)	−2.21

The energy of formation of poly(TAPP–Cu) is comparable with the energy of the porous Cu/TAPP surface coordination network (−2.40 eV molecule^{-1}), thus potentially compensating for the thermodynamic driving force. However, we believe that the stability of the adatom-coordinated poly(TAPP–Cu) chains is underestimated because the theoretical model involved periodic boundary conditions; in other words, the chain has been forced into a structure that is commensurate with the Cu substrate. Furthermore, the entropy contribution to the overall processes, which is not taken into account in our ground-state DFT calculations, is expected to contribute significantly to the thermodynamic driving force governing the chain formation.

The nitrogen atoms in the three chain structures of poly(iso-TAPP), poly(TAPP) and poly(TAPP–Cu) possess chemically different environments, which furthermore differ from the chemical environment in the porous Cu/TAPP network, from which the chains are chemically derived. Therefore, we employed XPS to characterise the polymeric chains further and to differentiate between the three structural models. Being a non-local, laterally averaging technique, XPS is especially suitable for determining the dominating type of chain in this case. The XPS data presented in our original communication on the chain formation[19] could be reproduced with high accuracy (and improved signal-to-noise ratio) by using synchrotron radiation (see Figure 9). However, on the basis of the preceding structural discussion as well as the theoretical modelling of chemical XPS shifts presented in this section (see below), we had to reconsider our original interpretation of the data.[19]

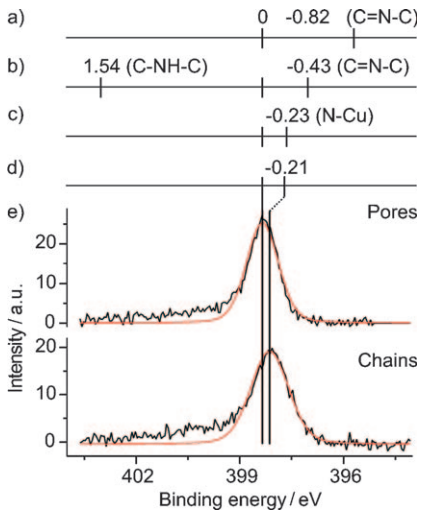

Figure 9. Calculated chemical shifts by using a core-ionised potential for a) poly(TAPP), b) poly(iso-TAPP) and c) poly(TAPP–Cu). d) Chemical shift of the porous network and the chains, determined from the fits of e) the XPS N1s spectra. All chemical shifts are referenced to the N1s peak of the porous Cu/TAPP network.

© 2010 Wiley-VCH Verlag GmbH & Co. KGaA, Weinheim

In the XPS N1s spectrum of the porous surface coordination network Cu/TAPP (Figure 9e, top), the single peak is consistent with the chemical equivalence of all the N-donor atoms in the quasi-tetragonal 2D coordination polymer. After annealing and formation of the irregular surface assemblies of covalent chains, this XPS peak is slightly broadened and shifted by −0.21 eV (Figure 9e, bottom). Given the quality of the data, it is assumed that this spectrum also corresponds to a single N-atom environment. This is consistent with either poly(TAPP) or poly(TAPP−Cu) as major components in the chain-structured organic material observed on the Cu(111) surface after annealing at >200 °C. Furthermore, the similarity of the peak energies before and after thermolysis of the Cu/TAPP surface network supports similar overall chemical environments of the N atoms in both cases. This supports our model of the Cu-decorated polymer chains poly(TAPP−Cu), an interpretation which has also been borne out by a theoretical modelling of the XPS N1s chemical shifts as indicated in Figure 9 above the two spectra.

The calculation of the XPS N1s data by DFT methods was carried out both by the $Z+1$ approximation and by the more accurate method by using a core-ionised potential; both approximations gave very similar results (Table 2).

Table 2. Calculated chemical shifts for the different types of chains by using two different approaches.[a]

Type of chain	$Z+1$ [eV]	Core-ionised potential [eV]
poly(iso-TAPP)		
C−N=C	−0.43	−0.43
C−NH−C	1.71	1.54
poly(TAPP) (C=N−C)	−0.87	−0.82
poly(TAPP−Cu) (N−Cu)	−0.23	−0.23

[a] The reference is the N1s peak of the porous network.

Comparison of the calculated shifts (Figure 9a–c) with the experimental results (Figure 9d and e) illustrates excellent agreement between the calculated chemical shift of the adatom-coordinated chain poly(TAPP−Cu) and the XPS spectra determined experimentally after annealing. This is consistent with the comparison of the XPS N1s chemical shifts before and after thermolysis discussed above and confirms the reaction-energy-based line of argument for the copper coordination put forward in the previous section (Table 1).

Good agreement between experimental results and theoretical studies was also observed for the simulation of STM images of the chains at low voltages (Figure 10). However, a distinction purely by STM between the different chain structures discussed in this work was not possible. The simulated STM images of the poly(iso-TAPP) chain (Figure 10c) and a poly(TAPP−Cu) chain (Figure 10a) do not reveal any visible differences and both correspond well with the experimental high-resolution image (Figure 10b). Both simulated images exhibit a significant electron density between the TAPP monomers, as observed experimentally. This provides further evidence for covalent linkages between the monomers.

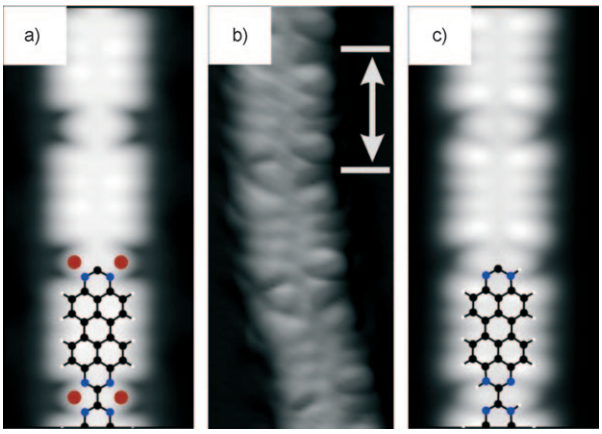

Figure 10. a) Simulated STM image of poly(TAPP−Cu). b) STM image of a TAPP chain in detail (1.8×4 nm^2, −0.6 V/20 pA), which corresponds well to the simulated STM images in (a) and (c). The distance between the monomers determined by STM was (1.23 ± 0.12) nm. c) Simulated STM image of poly(iso-TAPP). Both simulated STM images show the local density of states (LDOS) integrated from the Fermi level to −0.6 eV, thus corresponding to a constant-current image at −0.6 V.

The nature of inter-chain contacts: Closer inspection of the Cu(111) covered with the polymeric TAPP chains discussed above has revealed that there are manifold contacts between individual chains. In fact it appears that there is a certain tendency of the chains to form junctions at which the chain end of one oligomer connects to the side of another chain at the interstice between two monomeric units. An analysis of STM images obtained from samples at low (local) coverage indicates two major types of such junctions (Figure 11). Our interpretation of the chain structures as poly(TAPP−Cu) readily offers an explanation for these structural motifs, both of which are thought to be based on the assembly through Cu adatoms coordinated between two nitrogen atoms of adjacent monomers of one chain, while being ligated either to the carbene of the tautomerised chain end of the second molecule or to one of the nitrogen atoms of the pyrimidine end group in that species.

Both types can be distinguished by STM because their connecting angles are different (90° in the case illustrated in Figure 11d and 60° in the case in Figure 11e). Furthermore, detailed STM images show that the joining chain binds either along the principal molecular axis (Figure 11a) or off-centre (Figure 11b). Further support for our structural models is derived from the distances between distinctive points of the interacting chains determined by STM (as indicated in Figures 11a and b). These distances between the midpoints of the black dotted lines were found to be (16 ± 1.6) Å (Figure 11a) and (15 ± 1.5) Å (Figure 11b). They compare quite well with the values expected from the corresponding chemical models (17.0–17.8 Å and 16.1–16.8 Å) in which a Cu–C distance of 2.1 Å is used and the Cu–N distance may lie between 1.8 Å and 2.5 Å.

 © 2010 Wiley-VCH Verlag GmbH & Co. KGaA, Weinheim

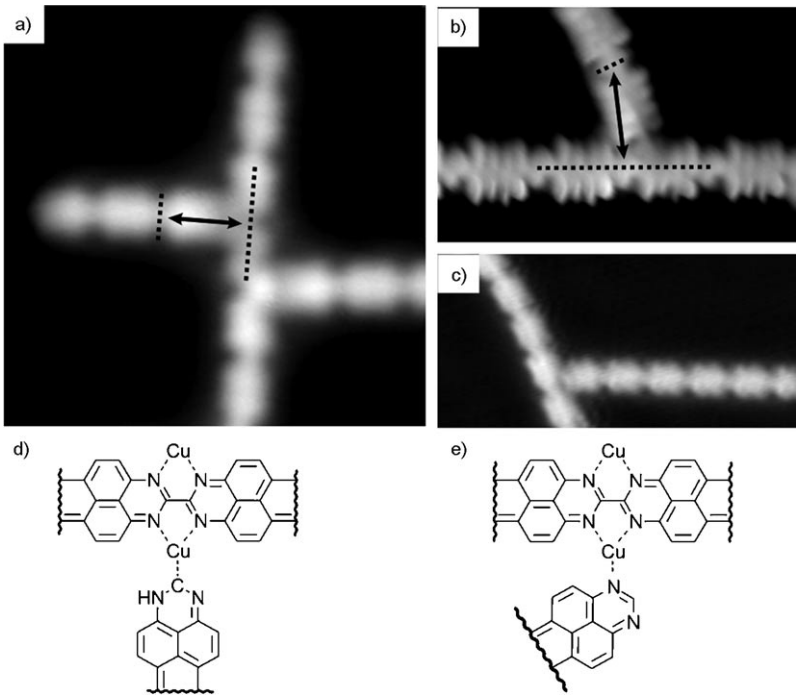

Figure 11. Different types of connections between chains. a) Image of a chain (7.3×7.3 nm^2, -1 V/20 pA) that typically attacks centrally between two monomers of another chain at an angle of approximately 90°. Second type: b) 4.8×3.1 nm^2, -0.6 V/20pA; c) (10.2×4.9 nm^2, 0.1 V/20pA). In this case, the chain coordinates slightly off-centre with variable angles between 60 and 70° which were determined by STM. d) Proposed structure of chain in (a). e) Proposed model corresponding to chains in (d). The distances between the midpoints of the black dotted lines in (a) and (b) determined by STM were (16 ± 1.6) and (15 ± 1.5) Å, respectively.

Conclusion

The combination of experimental techniques (STM and XPS) and DFT calculations allowed a detailed study of the chemistry of 1,3,8,10-tetraazaperopyrene (TAPP) on Cu(111) under ultra-high-vacuum (UHV) conditions. Depending on the annealing temperature, TAPP forms three main assemblies, resulting from initial submonolayer coverages that are based on different intermolecular interactions: a close-packed assembly similar to a projection of the bulk structure of TAPP in which the molecules interact mainly through vdW forces and weak H bonds; a porous copper surface coordination network; and covalently linked molecular chains (Figure 12).

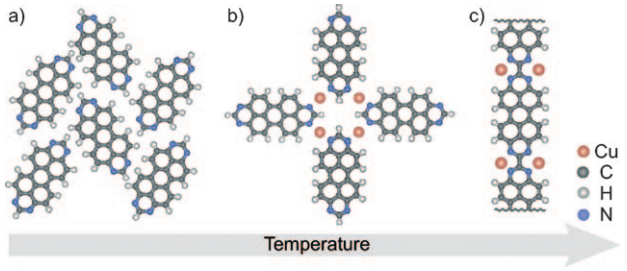

Figure 12. Thermal regimes of the assembly of TAPP on Cu(111): from a) vdW interaction through b) Cu coordination to c) covalent bonds.

The Cu substrate is crucially important in determining the structures of the aggregates and available reaction channels on the surface. This especially applies for the formation of the porous network for which it provides the Cu atoms for surface metal coordination. It equally applies to the covalent coupling of the TAPP molecules at higher temperatures. Here the Cu surface and its adatoms are thought to act catalytically for reaction pathways that are inaccessible in the bulk and for the stabilisation of reactive intermediates before they recombine.

Apart from their role in the kinetics of surface transformations, the available metal adatoms may also influence the thermodynamics of transformations profoundly, for example, by coordination to the reaction product as shown in this work for the case of the Cu-decorated covalent poly(TAPP–Cu) chains. This adds a further dimension to the emerging conceptual framework of surface-confined chemistry involving large organic molecules as structural (and potential functional) building blocks.[2,13]

Experimental Section

General surface analytical methods and procedures: The experiments were performed in a UHV system consisting of different chambers for sample preparation and characterisation, at a base pressure of 10^{-10} mbar. The Cu(111) single crystal was prepared by subsequent cycles of sputtering with Ar^+ ions and annealing at approximately 500 °C. TAPP[20] was deposited on the metal surface from a glass crucible that was heated inside a commercial evaporator (Kentax UHV equipment) while the rate was controlled by a quartz crystal microbalance (QMB).

The STM images have been acquired by using a commercial Omicron low-temperature scanning tunnelling microscope (LT-STM, Omicron NanoTechnology GmbH) operated at either 77 K or 5 K and equipped with wire-cut PtIr tips. The STM was operated by the Nanonis SPM control system (SPECS GmbH). In the experiments the bias voltage was applied to the tip. However, the bias voltages given in this manuscript refer to an grounded tip. For the molecular deposition the sample could be held at temperatures below (cooled by liquid nitrogen) or above RT. The annealing processes were initiated at temperatures well below the critical temperatures at which complete phase transformation occurred. After reaching the annealing temperature the sample was cooled down and studied with STM. The free software WSxM was used for data processing.[42]

The unit-cell size of the porous TAPP network was determined accurately by making LEED measurements. The LEED patterns were taken

 © 2010 Wiley-VCH Verlag GmbH & Co. KGaA, Weinheim

from samples held at room temperature. The sample was tilted slightly with respect to normal incidence to provide better visibility of the first-order diffraction spots that would otherwise interfere with the electron gun. LEEDpat 2.1 software was used to simulate the LEED pattern.[25]

For XPS measurements performed at beamline ID32 at the European Synchrotron Radiation Facility (ESRF) in Grenoble, synchrotron radiation tuned at an energy of approximately 2.97 keV was used. In the experimental set-up, the incident X-ray beam struck the surface (that is, the (111) plane) at approximately 90°. Time-dependent studies of the N1s peak indicated how and especially when the peaks were affected by the beam. On the basis of these studies a reasonable time frame was chosen to avoid beam damage.

Computational Studies

All calculations were done within the framework of DFT with periodic boundary conditions by using the Vienna Ab-initio Simulation Package (VASP).[43] The ion–core interaction was described by the projector augmented wave method.[44] The generalised gradient approximation (GGA) through the Perdew–Wang 91 (PW91) functional[45] was used to describe the exchange-correlation effects. The plane-wave basis was expanded up to a cut-off energy of 400 eV. Structural optimisation was performed with the conjugate gradient algorithm until the force on each atom was less than 0.01 eV Å^{-1}. The copper substrate was modelled by a four-layer slab separated by a vacuum region of seven times the lattice spacing; the two outermost copper layers were fully relaxed. A 2×2 k-point and 2×1 k-point sampling was used for the porous network and the chains, respectively.

The adsorption energies E_{ads} of the porous network (with or without adatoms) were calculated from Equation (1), in which $E_{pore(TAPP)/Cu(111)}$ is the total energy of the relaxed system of TAPP molecules (with or without adatoms) on the Cu(111) surface, E_{TAPP} is the total energy of the relaxed TAPP molecule and $E_{Cu(111)}$ is the total energy of the relaxed Cu(111) substrate including the adatoms if present in the porous network.

$$E_{ads} = \frac{1}{2}\left[E_{pore(TAPP)/Cu(111)} - \left(2E_{TAPP} - E_{Cu(111)}\right)\right] \quad (1)$$

The unit cell of the porous network contains two TAPP molecules (and four adatoms). For the tautomerised TAPP chain the reaction energies E_{react} were calculated by applying Equation (2), in which $E_{poly(xTAPP)/Cu(111)}$ is the total energy of the respective TAPP chain on Cu(111), and E_{TAPP} and $E_{Cu(111)}$ are defined as for the porous network.

$$E_{react} = E_{poly(xTAPP)/Cu(111)} - \left(E_{TAPP} + E_{Cu(111)}\right) + 2\left(E_{H/Cu(111)} - E_{Cu(111)}\right) \quad (2)$$

The last term, including $E_{H/Cu(111)}$, which is the total energy of atomic hydrogen on Cu(111), is added only for poly(TAPP) and poly(TAPP–Cu), and compensates for the two hydrogen atoms per TAPP molecule that are being adsorbed on the Cu(111) surface in the dehydrogenation process.

The Tersoff–Hamann approximation[46] was applied to calculate STM images, with the tunnelling current taken to be proportional to the integrated local density of states. The method used to evaluate the local density of states is described by Sacks et al.[47]

Core-level binding energies were calculated as the energy difference between two separate calculations: the first was a standard DFT calculation that gave the total energy of the system in its ground state; in the second, one electron was removed from the core of a particular atom. Core-level shifts were calculated by comparing total energy differences between core-ionised and ground-state systems. The total energies of the core-ionised systems were approximated in two ways, either 1) by using a core-ionised potential for the core-ionised atom as described by Köhler and Kresse,[48] or 2) by replacing the core-ionised atom with the next atom in the periodic table as described by the $Z+1$ approximation.[49]

Crystal structure analysis of TAPP: Long needles of TAPP were obtained by sublimation in a temperature-programmed tube furnace (440→250 °C) at ambient pressure under a stream of nitrogen as the carrier gas (diameter 33 mm; flow rate 15 L h^{-1}).

Crystal data: TAPP; $C_{22}H_{10}N_4$; monoclinic; space group $P2_1/c$; a = 3.7080(2), b = 11.2525(6), c = 16.6569(8) Å; β = 97.404(1)°; V = 689.20(6) Å^3; Z = 2; μ = 0.098 mm^{-1}; F_{000} = 340; θ range 2.2–32.0°; index ranges h,k,l (independent set): 0–5, 0–16, −24 to 23; 34 441 measured reflections; 2331 independent reflections; R_{int} = 0.0364; 1915 observed reflections [$I > 2\sigma(I)$]; final R indices [$F_o > 4\sigma(F_o)$] $R(F)$ = 0.0503; $wR(F^2)$ = 0.1485; $GooF$ = 1.094. Intensity data were collected at 100 K with a Bruker AXS Smart 1000 CCD diffractometer ($Mo_{K\alpha}$ radiation, graphite monochromator, λ = 0.710 73 Å). Data were corrected for air and detector absorption, and Lorentz and polarisation effects;[50] absorption by the crystal was treated with a semi-empirical multi-scan method.[51,52]

The structure was solved by conventional direct methods[53,54] and refined by full-matrix least-squares methods based on F^2 against all unique reflections.[54,55] All non-hydrogen atoms were given anisotropic displacement parameters. Hydrogen atoms were located from difference Fourier syntheses and refined with isotropic displacement factors.

CCDC-747374 contains the supplementary crystallographic data for this paper. These data can be obtained free of charge from The Cambridge Crystallographic Data Centre via www.ccdc.cam.ac.uk/data_request/cif.

Acknowledgements

We thank the Swiss National Science Foundation, the European Union through the Marie Curie Research Training Network PRAIRIES (MRTN-CT-2006-035810) and the University of Heidelberg for funding, and acknowledge the award of a predoctoral fellowship to S.M. by the Landesgraduiertenförderung Baden-Württemberg (Promotionskolleg "Molekulare Sonden"). Support from the National Centre of Competence in Research (NCCR) "Nanoscale Science" and the Wolfermann Naegeli Stiftung for the acquisition of the low-temperature STM, the Swedish Research Council (VR), and both the University of Liverpool and the Swedish National Allocations Committee (SNAC) for allocation of computer resources, are also acknowledged. Specs Zürich and the Swiss Commission for Technology and Innovation (CTI) is acknowledged for fruitful collaboration on the STM/STS data acquisition system.

[1] For selected recent overviews covering various aspects of the field, see: a) J. V. Barth, G. Costantini, K. Kern, *Nature* **2005**, *437*, 671; b) K.-H. Ernst, *Top. Curr. Chem.* **2006**, *265*, 209; c) K. Müllen, J. P. Rabe, *Acc. Chem. Res.* **2008**, *41*, 511; d) D. Li, R. B. Kaner, *Science* **2008**, *320*, 1170; e) M. Treier, R. Fasel, *Chimia* **2009**, *63*, 122; f) J. A. A. W. Elemans, S. Lei, S. De Feyter, *Angew. Chem.* **2009**, *121*, 7434; *Angew. Chem. Int. Ed.* **2009**, *48*, 7298.

[2] a) J. Sakamoto, J. van Heijst, O. Lukin, A. D. Schlüter, *Angew. Chem.* **2009**, *121*, 1048; *Angew. Chem. Int. Ed.* **2009**, *48*, 1030; b) D. F. Perepichka, F. Rosei, *Science* **2009**, *323*, 216; c) A. Gourdon, *Angew. Chem.* **2008**, *120*, 7056; *Angew. Chem. Int. Ed.* **2008**, *47*, 6950.

[3] Selected key references: a) C. Joachim, J. K. Gimzewski, A. Aviram, *Nature* **2000**, *408*, 541; b) C. D. Dimitrakopoulos, P. R. L. Malenfant, *Adv. Mater.* **2002**, *14*, 99; c) L. Venkataraman, J. E. Klare, C. Nuckolls, M. S. Hybertsen, M. L. Steigerwald, *Nature* **2006**, *442*, 904; d) B. Crone, A. Dodabalapur, Y.-Y. Lin, R. W. Filas, Z. Bao, A. LaDuca, R. Sarpeshkar, H. E. Katz, W. Li, *Nature* **2000**, *403*, 521; e) L. Fu, L. Cao, Y. Liu, D. Zhu, *Adv. Colloid Interface Sci.* **2004**, *111*, 133.

[4] a) J.-M. Lehn, *Supramolecular Chemistry—Concepts and Perspectives*, VCH, Weinheim, **1995**. See also: b) J.-M. Lehn, *Science* **2002**, *295*, 2400; c) O. Ikkala, G. ten Brinke, *Science* **2002**, *295*, 2407; d) D. N. Reinhoudt, M. Crego-Calama, *Science* **2002**, *295*, 2403; e) G. M. Whitesides, B. Grzybowski, *Science* **2002**, *295*, 2418; f) M. D. Hollingsworth, *Science* **2002**, *295*, 2410; g) T. Kato, *Science*

 © 2010 Wiley-VCH Verlag GmbH & Co. KGaA, Weinheim

2002, *295*, 2414; h) M. Ruben, J. Rojo, F. J. Romero-Salguero, L. H. Uppadine, J.-M. Lehn, *Angew. Chem.* **2004**, *116*, 3728; *Angew. Chem. Int. Ed.* **2004**, *43*, 3644.

[5] Selected examples: SPM: a) G. Binnig, H. Rohrer, *Rev. Mod. Phys.* **1987**, *59*, 615; b) F. J. Giessibl, *Rev. Mod. Phys.* **2003**, *75*, 949. Photoelectron spectroscopy: c) S. Hüfner, *Photoelectron Spectroscopy—Principles and Applications*, Springer, Heidelberg, **2003**. General overview of surface science techniques: d) K. Oura, V. G. Lifshits, A. A. Saranin, A. V. Zotov, M. Katayama, *Surface Science: An Introduction*, Springer, Berlin **2003**.

[6] a) R. Lazzaroni, A. Calderone, J. L. Brédas, J. P. Rabe, *J. Chem. Phys.* **1997**, *107*, 99; b) M. Elstner, D. Porezag, G. Jungnickel, J. Elsner, M. Haugk, T. Frauenheim, S. Suhai, G. Seifert, *Phys. Rev. B* **1998**, *58*, 7260; c) X. Wu, M. C. Vargas, S. Nayak, V. Lotrich, G. Scoles, *J. Chem. Phys.* **2001**, *115*, 8748; d) W. A. Hofer, A. S. Foster, A. L. Shluger, *Rev. Mod. Phys.* **2003**, *75*, 1287.

[7] a) J. V. Barth, *Annu. Rev. Phys. Chem.* **2007**, *58*, 375; b) L. Grill, *J. Phys. Condens. Matter* **2008**, *20*, 053001; c) S. Stepanow, N. Lin, J. V. Barth, *J. Phys. Condens. Matter* **2008**, *20*, 184002; d) A. Kühnle, *Curr. Opin. Colloid Interface Sci.* **2009**, *14*, 157.

[8] a) S. De Feyter, F. C. De Schryver, *Chem. Soc. Rev.* **2003**, *32*, 139; b) S. De Feyter, F. C. De Schryver, *J. Phys. Chem. B* **2005**, *109*, 4290; c) L.-J. Wan, *Acc. Chem. Res.* **2006**, *39*, 334; d) S. Yoshimoto, *Bull. Chem. Soc. Jpn.* **2006**, *79*, 1167; e) U. Ziener, *J. Phys. Chem. B* **2008**, *112*, 14698.

[9] a) F. Rosei, M. Schunack, Y. Naitoh, P. Jiang, A. Gourdon, E. Laegsgaard, I. Stensgaard, C. Joachim, F. Besenbacher, *Prog. Surf. Sci.* **2003**, *71*, 95; b) F. S. Tautz, *Prog. Surf. Sci.* **2007**, *82*, 479.

[10] a) M. Böhringer, K. Morgenstern, W.-D. Schneider, R. Berndt, F. Mauri, A. D. Vita, R. Car, *Phys. Rev. Lett.* **1999**, *83*, 324; b) S. Ito, M. Wehmeier, J. D. Brand, C. Kubel, R. Epsch, J. P. Rabe, K. Müllen, *Chem. Eur. J.* **2000**, *6*, 4327; c) T. Yokoyama, S. Yokoyama, Y. Okuno, S. Mashiko, *Nature* **2001**, *413*, 619; d) A. Langner, S. L. Tait, N. Lin, C. Rajadurai, M. Ruben, K. Kern, *Proc. Natl. Acad. Sci. USA* **2007**, *104*, 17927.

[11] a) J. Weckesser, A. D. Vita, J. V. Barth, C. Cai, K. Kern, *Phys. Rev. Lett.* **2001**, *87*, 096101; b) H. Spillmann, A. Dmitriev, N. Lin, P. Messina, J. V. Barth, K. Kern, *J. Am. Chem. Soc.* **2003**, *125*, 10725; c) M. de Wild, S. Berner, H. Suzuki, H. Yanagi, D. Schlettwein, S. Ivan, A. Baratoff, H.-J. Güntherodt, T. A. Jung, *ChemPhysChem* **2002**, *3*, 881; d) S. De Feyter, M. Larsson, N. Schuurmans, B. Verkuijl, G. Zoriniants, A. Gesquière, M. M. Abdel-Mottaleb, J. van Esch, B. L. Feringa, J. van Stam, F. De Schryver, *Chem. Eur. J.* **2003**, *9*, 1198; e) D. Bonifazi, H. Spillmann, A. Kiebele, M. de Wild, P. Seiler, F. Cheng, H.-J. Güntherodt, T. Jung, F. Diederich, *Angew. Chem.* **2004**; *Angew. Chem. Int. Ed.* **2004**, 43, 4759; f) M. E. Cañas-Ventura, W. Xiao, D. Wasserfallen, K. Müllen, H. Brune, J. V. Barth, R. Fasel, *Angew. Chem.* **2007**, *119*, 1846; *Angew. Chem. Int. Ed.* **2007**, *46*, 1814.

[12] Selected references: a) J. A. Theobald, N. S. Oxtoby, M. A. Phillips, N. R. Champness, P. H. Beton, *Nature* **2003**, *424*, 1029. See also: b) F. Cicoira, C. Santato, F. Rosei, *Top. Curr. Chem.* **2008**, *285*, 203; c) A. Ziegler, W. Mamdouh, A. Ver Heyen, M. Surin, H. Ujii, M. M. S. Abdel-Mottaleb, F. C. De Schryver, S. De Feyter, R. Lazzaroni, S. Höger, *Chem. Mater.* **2005**, *17*, 5670; d) S. Griessl, M. Lackinger, M. Edelwirth, M. Hietschold, W. M. Heckl, *Single Mol.* **2002**, *3*, 25; e) G. Pawin, K. L. Wong, K.-Y. Kwon, L. Bartels, *Science* **2006**, *313*, 961; f) H. Spillmann, A. Kiebele, M. Stöhr, T. A. Jung, D. Bonifazi, F. Cheng, F. Diederich, *Adv. Mater.* **2006**, *18*, 275; g) M. Wahl, M. Stöhr, H. Spillmann, T. A. Jung, L. H. Gade, *Chem. Commun.* **2007**, 1349; h) U. Schlickum, R. Decker, F. Klappenberger, G. Zoppellaro, S. Klyatskaya, M. Ruben, I. Silanes, A. Arnau, K. Kern, H. Brune, J. V. Barth, *Nano Lett.* **2007**, *7*, 3813; i) S. Furukawa, H. Ujii, K. Tahara, T. Ichikawa, M. Sonoda, F. C. De Schryver, Y. Tobe, S. De Feyter, *J. Am. Chem. Soc.* **2006**, *128*, 3502; j) M. Stöhr, M. Wahl, H. Spillmann, L. H. Gade, T. A. Jung, *Small* **2007**, *3*, 1336; k) S. Lei, K. Tahara, X. Feng, S. Furukawa, F. C. De Schryver, K. Müllen, Y. Tobe, S. De Feyter, *J. Am. Chem. Soc.* **2008**, *130*, 7119.

[13] Recent reviews: a) N. Lin, S. Stepanow, M. Ruben, J. V. Barth, *Top. Curr. Chem.* **2009**, *275–278*, 1; b) J. V. Barth, *Surf. Sci.* **2009**, *603*, 1533.

[14] Selected examples: a) A. Dmitriev, H. Spillmann, N. Lin, J. V. Barth, K. Kern, *Angew. Chem.* **2003**, *115*, 2774; *Angew. Chem. Int. Ed.* **2003**, *42*, 2670; b) M. A. Lingenfelder, H. Spillmann, A. Dmitriev, S. Stepanow, N. Lin, J. V. Barth, K. Kern, *Chem. Eur. J.* **2004**, *10*, 1913; c) N. Lin, S. Stepanow, F. Vidal, J. V. Barth, K. Kern, *Chem. Commun.* **2005**, 1681; d) T. Classen, G. Fratesi, G. Costantini, S. Fabris, F. Stadler, C. Kim, S. de Gironcoli, S. Baroni, K. Kern *Angew. Chem.* **2005**, *117, 6298; Angew. Chem. Int. Ed.* **2005**, 44, 6142; *Angew. Chem. Int. Ed.* **2005**, *44*, 6142; e) N. Lin, S. Stepanow, F. Vidal, K. Kern, M. S. Alam, S. Strömsdörfer, V. Dremov, P. Müller, A. Landa, M. Ruben, *Dalton Trans.* **2006**, 2794; f) S. Stepanow, N. Lin, D. Payer, U. Schlickum, F. Klappenberger, G. Zoppellaro, M. Ruben, H. Brune, J. V. Barth, K. Kern, *Angew. Chem.* **2007**, *119*, 724; *Angew. Chem. Int. Ed.* **2007**, *46*, 710; g) S. Tait, A. Langner, N. Lin, S. Stepanow, C. Rajadurai, M. Ruben, K. Kern, *J. Phys. Chem. C* **2007**, *111*, 10982; h) A. Langner, S. L. Tait, N. Lin, R. Chandrasekar, M. Ruben, K. Kern, *Angew. Chem.* **2008**, *120*, 8967; *Angew. Chem. Int. Ed.* **2008**, *47*, 8835; i) S. L. Tait, A. Langner, N. Lin, R. Chandrasekar, M. Ruben, K. Kern, *ChemPhysChem* **2008**, *9*, 2594; j) D. Kühne, F. Klappenberger, R. Decker, U. Schlickum, H. Brune, S. Klyatskaya, M. Ruben, J. V. Barth, *J. Am. Chem. Soc.* **2009**, *131*, 3881; k) A. Langner, S. Tait, N. Lin, R. Chandrasekar, M. Ruben, K. Kern, *Chem. Commun.* **2009**, 2502.

[15] R. F. W. Bader, *Atoms in Molecules—A Quantum Theory*, Clarendon Press, Oxford, **1994**.

[16] a) S. W. Hla, L. Bartels, G. Meyer, K. H. Rieder, *Phys. Rev. Lett.* **2000**, *85*, 2777; b) Y. Okawa, M. Aono, *Nature* **2001**, *409*, 683; c) H. Ozaki, T. Funaki, Y. Mazaki, S. Masuda, Y. Harada, *J. Am. Chem. Soc.* **1995**, *117*, 5596.

[17] a) S. Weigelt, C. Busse, C. Bombis, M. M. Knudsen, K. V. Gothelf, T. Strunskus, C. Wöll, M. Dahlboom, B. Hammer, E. Laegsgaard, F. Besenbacher, T. R. Linderoth, *Angew. Chem.* **2007**, *119*, 9387; *Angew. Chem. Int. Ed.* **2007**, *46*, 9227; b) N. A. A. Zwaneveld, R. Pawlak, M. Abel, D. Catalin, D. Gigmes, D. Bertin, L. Porte, *J. Am. Chem. Soc.* **2008**, *130*, 6678; c) S. Boz, M. Stöhr U. Soydaner, M. Mayor, *Angew. Chem.* **2009**, *121*, 3225; *Angew. Chem. Int. Ed.* **2009**, *48*, 3179; d) C. H. Schmitz, J. Ikonomov, M. Sokolowski, *J. Phys. Chem. C* **2009**, *113*, 11984.

[18] a) L. Grill, M. Dyer, L. Lafferentz, M. Persson, M. V. Peters, S. Hecht, *Nat. Nanotechnol.* **2007**, *2*, 687; b) M. In't Veld, P. Iavicoli, S. Haq, D. B. Amabilino, R. Raval, *Chem. Commun.* **2008**, 1536.

[19] M. Matena, T. Riehm, M. Stöhr, T. A. Jung, L. H. Gade, *Angew. Chem.* **2008**, *120*, 2448; *Angew. Chem. Int. Ed.* **2008**, *47*, 2414.

[20] T. Riehm, G. DePaoli, A. Konradsson, L. de Cola, H. Wadepohl, L. H. Gade, *Chem. Eur. J.* **2007**, *13*, 7317.

[21] a) G. R. Desiraju, A. Gavezotti, *Acta Crystallogr. Sect. B* **1989**, *45*, 473; G. R. Desiraju, A. Gavezotti, *J. Chem. Soc. Chem. Commun.* **1989**, 621; b) D. M. Cho, S. R. Parkin, M. D. Watson, *Org. Lett.* **2005**, *7*, 1067; c) C. A. Hunter, K. R. Lawson, J. Perkins, C. J. Urch, *J. Chem. Soc. Perkin Trans. 2* **2001**, 651; d) M. D. Curtis, J. Cao, J. W. Kampf, *J. Am. Chem. Soc.* **2004**, *126*, 4318; e) G. Horowitz, B. Bachet, A. Yassar, P. Lang, F. Demanze, J.-L. Fave, F. Garnier, *Chem. Mater.* **1995**, *7*, 1337; f) D. Fichou, *J. Mater. Chem.* **2000**, *10*, 571.

[22] a) G. R. Desiraju, T. Steiner, *The Weak Hydrogen Bond in Structural Chemistry and Biology*, Oxford University Press, New York, **1999**; b) M. Mascal, *Chem. Commun.* **1998**, 303; c) F. A. Cotton, L. M. Daniels, G. T. Jordan IV, C. A. Murillo, *Chem. Commun.* **1997**, 1673; d) R. Taylor, O. Kennard, *J. Am. Chem. Soc.* **1982**, *104*, 5063; e) V. R. Thalladi, A. Gehrke, R. Boese, *New J. Chem.* **2000**, *24*, 463; f) R. Cini, C. Bellucci, G. Tamasi, M. Corsini, M. Fontani, P. Zanello, *Inorg. Chim. Acta* **2002**, *339*, 89; g) M. Hartmann, L. Radom, *J. Phys. Chem. A* **2000**, *104*, 968.

[23] a) R. E. Franklin, *Acta Crystallogr.* **1951**, *4*, 253; b) G. E. Bacon, *Acta Crystallogr.* **1951**, *4*, 458.

 © 2010 Wiley-VCH Verlag GmbH & Co. KGaA, Weinheim

[24] K. Glöckler, C. Seidel, A. Soukopp, M. Sokolowski, E. Umbach, M. Böhringer, R. Berndt, W. D. Schneider, *Surf. Sci.* **1998**, *405*, 1.
[25] LEED pattern simulator: LEEDpat Version 2.1, K. Hermann, M. A. van Hove, **2006**.
[26] D. E. Hooks, T. Fritz, M. D. Ward, *Adv. Mater.* **2001**, *13*, 227.
[27] M. Giesen, *Surf. Sci.* **1999**, *442*, 543.
[28] a) F. H. Allen, O. Kennard, *Chem. Des. Autom. News* **1993**, *8*, 1631; b) D. A. Fletcher, R. F. McMeeking, D. J. Parkin, *J. Chem. Inf. Comput. Sci.* **1996**, *36*, 746. See also: L. H. Gade, *Koordinationschemie*, Wiley-VCH, Weinheim, **1998**.
[29] C. C. Perry, S. Haq, B. G. Frederick, N. V. Richardson, *Surf. Sci.* **1998**, *409*, 512.
[30] a) S. Stepanow, M. Lingenfelder, A. Dmitriev, H. Spillmann, E. Delvigne, N. Lin, X. Deng, C. Cai, J. V. Barth, K. Kern, *Nat. Mater.* **2004**, *3*, 229; b) S. Stepanow, N. Lin, J. V. Barth, K. Kern, *J. Phys. Chem. B* **2006**, *110*, 23472.
[31] J. V. Barth, J. Weckesser, N. Lin, A. Dmitriev, K. Kern, *Appl. Phys. A* **2003**, *76*, 645.
[32] N. Lin, A. Dmitriev, J. Weckesser, J. V. Barth, K. Kern, *Angew. Chem.* **2002**, *114*, 4973; *Angew. Chem. Int. Ed.* **2002**, *41*, 4779.
[33] a) M. Schunack, F. Rosei, Y. Naitoh, P. Jiang, A. Gourdon, E. Laegsgaard, I. Stensgaard, C. Joachim, F. Besenbacher, *J. Chem. Phys.* **2002**, *117*, 6259. A fundamental study on the energies controlling surface restructuring processes on Ag (111) has been published by Morgenstern et al.: b) K. Morgenstern, G. Rosenfeld, E. Laegsgaard, F. Besenbacher, G. Comsa, *Phys. Rev. Lett.* **1998**, *80*, 556.
[34] M. Giesen, *Prog. Surf. Sci.* **2001**, *68*, 1.
[35] M. Giesen, G. Icking-Konert, *Surf. Sci.* **1998**, *412–413*, 645.
[36] H.-W. Wanzlick, *Angew. Chem.* **1962**, *74*, 129; *Angew. Chem. Int. Ed. Engl.* **1962**, *1*, 75.
[37] Y. Hasegawa, P. Avouris, *Phys. Rev. Lett.* **1993**, *71*, 1071.
[38] M. F. Crommie, C. P. Lutz, D. M. Eigler, *Nature* **1993**, *363*, 524.
[39] a) E. Alvarez, S. Conejero, M. Paneque, A. Petronilho, M. L. Poveda, O. Serrano, E. Carmona, *J. Am. Chem. Soc.* **2006**, *128*, 13060; an analogous reaction has been reported for a quinoline derivative inter alia: b) M. Esteruelas, F. J. Fernández-Alvarez, E. Oñate, *J. Am. Chem. Soc.* **2006**, *128*, 13044; review: c) D. Kunz, *Angew. Chem.* **2007**, *119*, 3473; *Angew. Chem. Int. Ed.* **2007**, *46*, 3405.
[40] a) J. C. Y. Lin, R. T. W. Huang, C. S. Lee, A. Bhattacharyya, W. S. hwang, I. J. B. Lin, *Chem. Rev.* **2009**, *109*, 3561; b) S. Diez-Gonzalez, N. Marion, S. P. Nolan, *Chem. Rev.* **2009**, *109*, 3612; c) S. Díez-González, S. P. Nolan, *Acc. Chem. Res.* **2008**, *41*, 349; d) *N-Heterocyclic Carbenes in Syntheses* (Ed.: S. P. Nolan), Wiley-VCH, Weinheim, **2006**; e) S. P. Nolan, *Chem. Eur. J.* **2008**, *14*, 158; f) P. L. Arnold, *Heteroat. Chem.* **2002**, *13*, 534; g) C. Nolte, P. Mayer, B. F. Straub, *Angew. Chem.* **2007**, *119*, 2147; *Angew. Chem. Int. Ed.* **2007**, *46*, 2101.
[41] M. Stöhr, M. Wahl, C. H. Galka, T. Riehm, T. A. Jung, L. H. Gade, *Angew. Chem.* **2005**, *117*, 7560; *Angew. Chem. Int. Ed.* **2005**, *44*, 7394.
[42] I. Horcas, R. Fernández, J. M. Gómez-Rodríguez, J. Colchero, *Rev. Sci. Instrum.* **2007**, *78*, 013705.
[43] G. Kresse, J. J. Furthmüller, *Phys. Rev. B* **1996**, *54*, 11169.
[44] a) P. E. Blüchl, *Phys. Rev. B* **1994**, *50*, 17593; b) G. Kresse, D. Joubert, *Phys. Rev. B* **1999**, *59*, 1758.
[45] P. Perdew, J. A. Chevary, S. H. Vosko, K. A. Jackson, M. R. Pederson, D. J. Singh, C. Fiolhais, *Phys. Rev. B* **1992**, *46*, 6671.
[46] a) J. Tersoff, D. R. Hamann, *Phys. Rev. B* **1985**, *31*, 805; b) J. Tersoff, D. R. Hamann, *Phys. Rev. Lett.* **1983**, *50*, 1998.
[47] W. Sacks, S. Gauthier, S. Rousset, J. Klein, M. A. Erck, *Phys. Rev. B* **1987**, *36*, 961.
[48] L. Köhler, G. Kresse, *Phys. Rev. B* **2004**, *70*, 165405.
[49] B. Johansson, N. Mårtensson, *Phys. Rev. B* **1980**, *21*, 4427.
[50] SAINT, Bruker AXS, **1997–2008**.
[51] R. H. Blessing, *Acta Crystallogr. Sect. A* **1995**, *51*, 33.
[52] SADABS, G. M. Sheldrick, Bruker AXS, **2004–2008**.
[53] SHELXS-97, G. M. Sheldrick, University of Göttingen, Göttingen, **1997**.
[54] G. M. Sheldrick, *Acta Crystallogr. Sect. A* **2008**, *64*, 112.
[55] SHELXL-97, G. M. Sheldrick, University of Göttingen, Göttingen, **1997**.

Received: September 21, 2009
Published online: January 14, 2010

 © 2010 Wiley-VCH Verlag GmbH & Co. KGaA, Weinheim